High spin to low spin relaxation regime change in a multistep 3D spin-crossover material

Guillaume Chastanet, Natasha Sciortino, Suzanne Neville, Cameron Kepert

▶ **To cite this version:**

Guillaume Chastanet, Natasha Sciortino, Suzanne Neville, Cameron Kepert. High spin to low spin relaxation regime change in a multistep 3D spin-crossover material. European Journal of Inorganic Chemistry, 2018, Molecular Magnetism, 2018 (3-4), pp.314-319. 10.1002/ejic.201701127 . hal-01696992

HAL Id: hal-01696992
https://hal.science/hal-01696992

Submitted on 30 Jan 2018

HAL is a multi-disciplinary open access archive for the deposit and dissemination of scientific research documents, whether they are published or not. The documents may come from teaching and research institutions in France or abroad, or from public or private research centers.

L'archive ouverte pluridisciplinaire **HAL**, est destinée au dépôt et à la diffusion de documents scientifiques de niveau recherche, publiés ou non, émanant des établissements d'enseignement et de recherche français ou étrangers, des laboratoires publics ou privés.

DOI: 10.1002/ejic.200((will be filled in by the editorial staff))

High Spin → Low Spin Relaxation Regime Change in a Multistep 3D Spin-Crossover Material

Guillaume Chastanet,[a]* Natasha F. Sciortino,[b] Suzanne M. Neville,[b] Cameron J. Kepert[b]

This paper is dedicated to the memory of Professor Olivier Kahn and his infusive ideas.

Keywords: Multistep spin crossover / Iron(II) / relaxation kinetics / LIESST / Photomagnetism /

Abstract: The paper reports the study of photo-induced HS state lifetime in a multistep spin crossover compound. Despite the pronounced three step transition of the $[Fe(dpsme)Pt(CN)_4]\cdot\frac{2}{3}dpsme\cdot x EtOH\cdot y H_2O$ (dpsme = 4,4′-di(pyridylthio)methane; EtOH = ethanol) 3D compound, neither the *T*(LIESST) nor the relaxation kinetics exhibit stepwise features. From the detailed investigation (experiments and simulations) of these relaxations and the record of the light-induced thermal hysteresis, the occurrence of a phase transition around 58 K is suspected.

Introduction

The light-induced spin-crossover (SCO) phenomenon is widely investigated[1,2] since fast photoswitching can be achieved at room temperature,[3,4] leading to possible applications in nanoscience,[5] sensors[6,7] and other types of functional materials applications.[8,9] The most studied SCO ion is undoubtedly iron(II), since it can exhibit a diamagnetic (S = 0, low spin LS) to paramagnetic (S = 2, high spin, HS) transition under light, temperature, pressure, magnetic field or chemical perturbation. Upon this electronic change, structural reorganisations take place due to the metal-ligand bond-length change associated with the SCO[10]. Elastic interactions between SCO molecules organised into a crystallographic network can propagate these structural changes and might promote cooperative effects responsible of hysteretic behaviours. Such elastic interactions can be either ferroelastic-like, favouring the population of the same spin state, or antiferroelastic-like responsible of alternating LS/HS states. The elastic frustration resulting from the existence of both type of interactions leads to the occurrence of symmetry breaking in the materials[11]. It results in multistep spin crossover behaviours with an increasing number of reported examples.

The Light-Induced Excited Spin-State Trapping (LIESST) effect is probably the most studied photoswitching process. It involves the population of the HS metastable state that occurs at low temperature through excitation in the absorption bands of the LS state.[12] The lifetime of the photo-induced HS state by LIESST effect has been widely studied to probe the chemical levers that can be manipulated to tune the temperature range of observation of this metastable state. In that sense, the work of Hauser and collaborators[13-14] has been of central importance to understand the role of different physico-chemical parameters on the relaxation kinetics, including cooperativity. Correlation between the relaxation rate and thermal SCO temperature, $T_{1/2}$ have then been evidenced. The general trend is that higher $T_{1/2}$ values lead to a faster relaxation process. Moreover, employing the *T*(LIESST) procedure[15], the role of the coordination sphere distortion has been pointed out as favouring the light-induced HS state. This T(LIESST) temperature records the temperature at which the photo-induced HS state is erased (with a standardized warming protocol).[16-21] Of further importance, according to these correlations, when multistep SCO occurs it should be echoed in the *T*(LIESST) curve; as long as the steps are well-defined and separated. When multiple iron(II) sites are involved this is usually the case[22-24] but it becomes less systematic when symmetry breaking is involved in the stepped SCO.[25-30] The structural changes that occur during the thermal SCO at high temperature (between 70 and 400 K) are not necessarily mirrored in the light-induced process. When the metastable state exhibits a clear symmetry breaking upon relaxation, multistep isothermal relaxation curves are obtained. In the present study, we show that even in a well-defined three-step SCO material, the photo-induced state can exhibit unusual and unexpected behaviour, without usual stepped relaxation.

In this study we investigate in detail the LIESST properties of the 3D framework material $[Fe(dpsme)Pt(CN)_4]\cdot\frac{2}{3}dpsme\cdot x EtOH\cdot y H_2O$ (dpsme = 4,4′-di(pyridylthio)methane; EtOH = ethanol), **1**, which exhibits a three-step SCO transition that is unique in occurring both on cooling and warming and in having broad thermal hysteresis.[30] Accompanying this stepwise transition is a series of subtle structural modulations in which the material converts between different long-range configurations of ordered HS and LS sites. Several symmetry breaking transitions

[a] Guillaume Chastanet, *CNRS, Université de Bordeaux, ICMCB, 87 avenue du Dr. A. Schweitzer, Pessac, F-33608, France*
E-Mail : guillaume.chastanet@icmcb.cnrs.fr
http://www.icmcb-bordeaux.cnrs.fr/spip.php?rubrique85
[b] Natasha F. Sciortino, Suzanne M. Neville, Cameron J. Kepert, *School of Chemistry, The University of Sydney, Camperdown NSW 2006, Australia*

Supporting information for this article is available on the WWW under http://www.eurjic.org/ or from the author.

occur in tandem with the thermal SCO. This compound exhibits a reversible photo-switching at low temperature but apparently no evidence of phase transition on the *T*(LIESST) curve. The present study investigates in detail the lifetime of the photo-induced HS state to see whether or not some unexpected behaviours are hidden.

Results and Discussion

Thermo- and photo-induced spin crossover

The magnetic and photomagnetic properties of the title compound have already been reported[30] and are summarised here to facilitate a detailed discussion of the kinetics. Figure 1a reports the thermal SCO curve recorded on the sample. The observed three-step character has been studied from the crystallographic point of view, evidencing three successive symmetry breakings. The spin transition follows the *State 1* [HS] ← *Step 1* → *State 2* [1:1 HS:LS] ← *Step 2*→ *State 3* [*ca.* 1:2 HS:LS] ← *Step 3* → *State 4* [LS] process**.** Notably, the multiple steps are enclosed within a single thermal hysteresis loop.

The title compound also shows light-induced switching properties. Irradiation at 10 K of the LS state with green light (514 nm) induces a partial photoconversion to the HS state according to the LIESST effect.[12] This photo-induced HS state can be depopulated by irradiating at 830 nm according to the reverse-LIESST process.[30] A remarkable feature of this photo-reversibility is that the reverse-LIESST process is complete while the pathway through the triplet state is assumed to disfavour this quantitative HS state erasing. The relaxation temperature of the photo-induced state was determined using a conventional *T*(LIESST) procedure[17] in which the material was heated in the dark from 10 K at 0.3 K min^{-1}. Relaxation of the photo-induced state occurs above 50 K with a *T*(LIESST) temperature of 56 K. In contrast to the thermal SCO, no steps or intermediate phases are evidenced in the *T*(LIESST) curve.

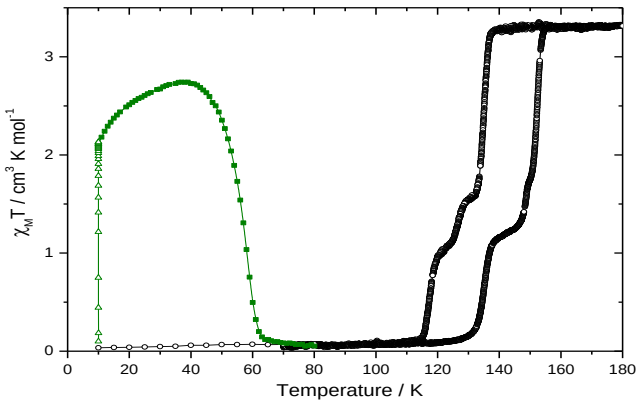

Figure 1: Thermal behaviour of the $\chi_M T$ product in the dark before irradiation (o) under irradiation at 532 nm (Δ), after irradiation in the dark (■).

Experimental relaxation curves

A complementary way to gain insight into the lifetime of the photo-induced HS state is to record relaxation kinetics at different temperatures. Figure 2 reports the recorded relaxation curves from 40 to 62 K. At 40 K the relaxation is relatively slow since only 20 % of the photo-induced state relaxes over a period of 12 hr. To extract the activation energy of the system the relaxation curves were modelled. A detailed inspection of these curves indicates that neither a simple exponential process nor a pure self-accelerated model reflect the experimental behaviour. Indeed, a single exponential fit fails to reproduce correctly the experimental curves (Figure 3a). The use of stretched or bi-exponential models does not improve the fit.

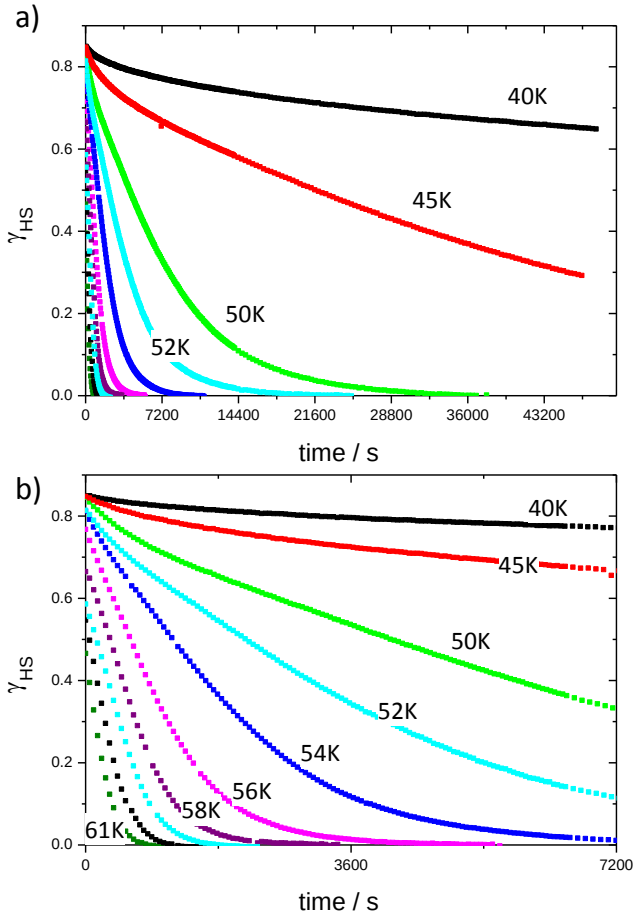

Figure 2: Relaxation kinetics of the photo-induced HS state at different temperatures from 40 to 60 K in (a,b).

This deviation from the single exponential behaviour can be simulated according to the self-accelerated process described by A. Hauser.[14-16] The use of such model that reflects the presence of cooperative interaction acting during the relaxation process could agree with the cooperative character of the thermal SCO. This model traduces a change in the energy barrier as a function of γ_{HS} (see Equations 1-4) where $\alpha(T) = (E_a^*/k_B T)$ is the acceleration factor at a given temperature and the relaxation rate $k^*_{HL}(T, \gamma_{HS})$ depends exponentially on both γ_{HS} and T (eq. (1) and (2)).

$$\frac{\partial \gamma_{HS}}{\partial t} = -k^*_{HL}\gamma_{HS} \quad (1)$$

$$k^*_{HL}(T, \gamma_{HS}) = k_{HL}(T).\exp[\alpha(T)(1-\gamma_{HS})] \quad (2)$$

$$k_{HL}(T) = k_\infty.\exp(-E_a / k_B T) \quad (3)$$

$$\frac{\partial \gamma_{HS}}{\partial t} = -\gamma_{HS}\left\{k_\infty . exp\left(-E_a/k_B T\right)\right\}. exp[\alpha(T)(1-\gamma_{HS})] \quad (4)$$

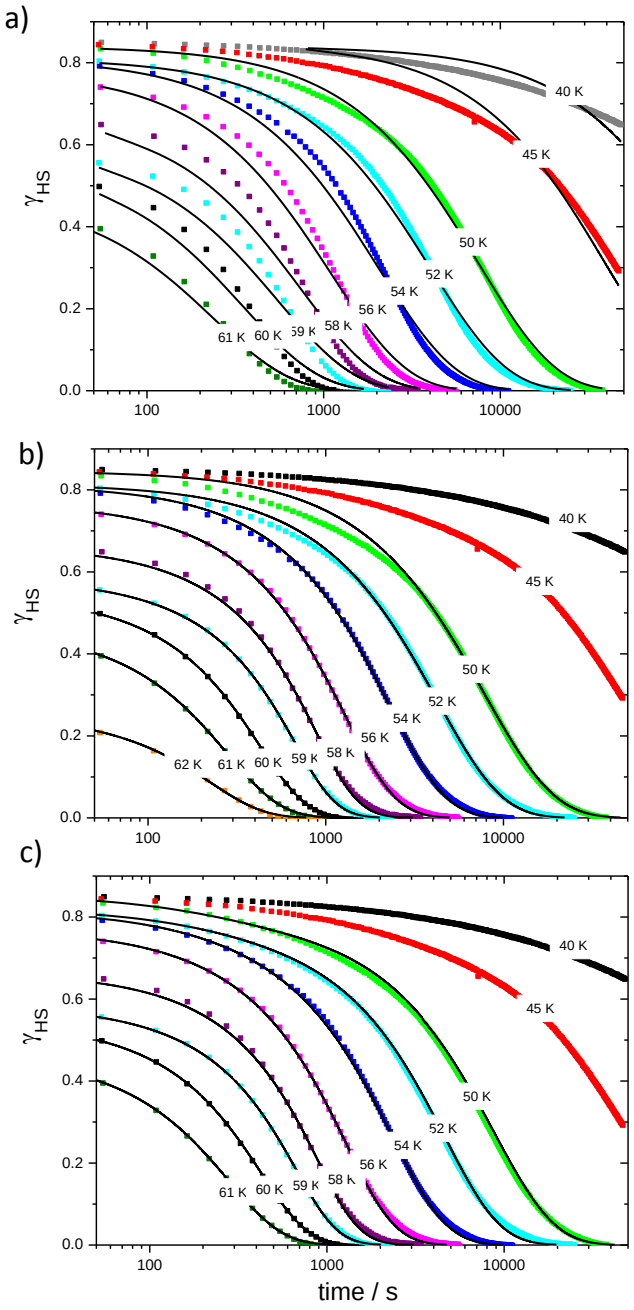

Figure 3: Relaxation of the photoinduced HS state at various temperatures after LIESST excitation at 10 K for **1**, with data points showing the experimental behaviour on a logarithm scale of the time. The lines of fit correspond to the simulation discussed in the text according to (a) single exponential fit, (c) self-accelerated simulation and (d) combination of exponential and self-accelerated relaxation.

Figure 3b reports the best simulations obtained using this procedure. From 61 K down to 56 K, the fit satisfactorily reproduces the experiment; however, a clear deviation appears at the beginning of the relaxation for lower temperatures (below 56 K). This deviation indicates the presence of a fast relaxing species. This fast relaxing fraction was modelled using a combination of w_1 exponential relaxation and w_2 self-accelerated process, with w_1+w_2 being equal to $\gamma_{HS}(t=0)$. Figure 3c reports the best simulations obtained using such approach and clearly shows the improvement brought by this combination compared to the previous simulations.

Deviations from classical self-accelerated behaviours have already been observed and explored. The presence of a small fast relaxing species at short time scale can follow from photo-excitation inhomogeneities. Due to the strong colour change upon spin change, bleaching effect can be involved in this photoswitching process, leading to differences in the population between the surface of the sample and the bulk [31]. In addition, defects in the sample or the presence of a relaxation process relative to a specific iron(II) site are not excluded. Finally, it has also been shown that short range and long-range interaction may co-exist in the same sample, giving rise to similar deviations [32].

From these successful simulations of the experimental relaxation kinetics, we can extract the relaxation rates at each temperature (Table 1) and the dynamical parameters of the system. This is conventionally achieved through an Arrhenius plot of lnk *vs* 1/T (Figure 4). In the present case, this plot reveals an original feature with a deviation from the expected linear behaviour occurring between 56 and 59 K. This deviation is observed either with the relaxation rates obtained from the single self-accelerated process or the combined exponential/self-accelerated processes. This comparison strongly limits the effect of over-parametrisation of the processes.

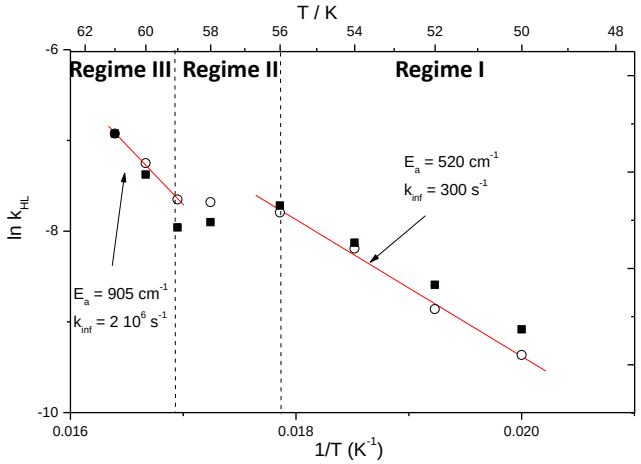

Figure 4: Thermal evolution of the relaxation rate ln k_{HL} extracted from the simple self-accelerated model (■) and the combination of exponential and self-accelerated relaxations (o).

At this level of investigation, it is impossible to certify if the exponential relaxing fraction and the two self-accelerated processes are related to the three-step character of the thermal SCO. A decrease in monocrystallinity arising with cycling through the photo-induced SCO transition prevented photo-crystallographic characterisation. The important point is that despite the cooperative 3 steps process of the thermal spin crossover, the relaxation curves do not exhibit such clear symmetry breaking. However, a change in the relaxation regime seems to occur around 56 K, whose origin cannot be identified for the moment. The dynamical parameters of the two relaxation processes were estimated from the linear fit of the regime I and regime III regions of the lnk *vs* 1/T plot (Figure 4): E_a = 520 cm^{-1}, $k(T\rightarrow\infty)$ = 300 s^{-1} and E_a* = 35 cm^{-1} for the species relaxing below 56 K (LT species) and E_a = 905 cm^{-1}, $k(T\rightarrow\infty) = 2\ 10^6$ s^{-1} and E_a* = 75 cm^{-1} for the species relaxing above 59 K (HT species). In regime II, different parameters could be extracted depending on the fitting procedure used. The main observation is related to the almost temperature independent character of this regime, which is usually observed in the tunneling region[13], and is therefore surprising in

Table 1 Results of the different simulations performed according to the models described in the text.

	exponential	sigmoid		exponential + sigmoid		
T (K)	**(w)[(1)] k (s^{-1})**	**k (s^{-1})**	**α / E_a*(cm^{-1})**	**(w1) k_{exp} (s^{-1})**	**(w2) k_{sig} (s^{-1})**	**α / E_a*(cm^{-1})**
40	(0.85) 7.24×10^{-6}	-	-			
45	(0.85) 2.56×10^{-5}	-	-			
50	(0.84) 1.32×10^{-4}	1.14×10^{-4}	0.32 / 11	(0.055) 4.5×10^{-3}	(0.945) 8.57×10^{-5}	0.74 / 25
52	(0.81) 2.48×10^{-4}	1.86×10^{-4}	0.58 / 21	(0.040) 5.00×10^{-3}	(0.960) 1.42×10^{-4}	1.03 / 37
54	(0.81) 4.87×10^{-4}	2.95×10^{-4}	0.97 / 36	(0.025) 5.50×10^{-3}	(0.975) 2.77×10^{-4}	1.07 / 40
56	(0.78) 9.12×10^{-4}	4.45×10^{-4}	1.29 / 50	(0.010) 6.50×10^{-3}	(0.990) 4.12×10^{-4}	1.44 / 56
58	(0.68) 1.36×10^{-3}	3.71×10^{-4}	1.90 / 76	-	(1.0) 3.71×10^{-4}	1.90 / 76
59	(0.60) 1.82×10^{-3}	3.49×10^{-4}	2.00 / 82	-	(1.0) 3.49×10^{-4}	2.00 / 82
60	(0.56) 2.86×10^{-3}	6.26×10^{-4}	2.00 / 83	-	(1.0) 6.26×10^{-4}	2.00 / 83
61	(0.48) 4.21×10^{-3}	9.83×10^{-4}	1.94 / 82	-	(1.0) 9.83×10^{-4}	1.94 / 82

[(1)] A weight ratio was applied to account for the fact that the relaxation curves do not start from $\gamma_{HS} = 1$

the middle of a relaxation process. This regime change more probably reflects a change in the relaxing entities (structural change, symmetry breaking…) that could not be identified at the moment.

All these considerations being taken, the extracted thermodynamic parameters can be used to simulate the *T*(LIESST) curve. Starting from the parameters obtained below 56 K (LT species) or above 59 K (HT species), two curves are simulated (Figure 5). While the parameters differ greatly, the curves are very close to each other. The main difference lies in the cooperative character of the HS→LS relaxation that is higher using the HT species parameters. This proximity of the two simulated curves explains the absence of steps in the *T*(LIESST) curves since the two processes have almost simultaneous relaxation rates despite their different thermodynamic characteristics. Moreover, a global and precise simulation of the *T*(LIESST) curve is not feasible since the assumed phase transition would correspond to an unknown fraction of the sample, with a coexistence of the two processes over several degrees. Nevertheless, Figure 5 shows that the *T*(LIESST) is mainly governed by the LT species behaviour since the corresponding simulated curve is very close to the experimental one.

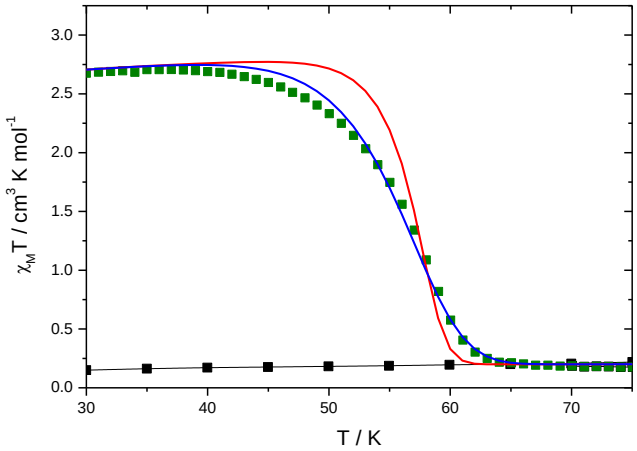

Figure 5: *T*(LIESST) simulations compared to the experimental curve (squares). The blue curve has been simulated with E_a = 520 cm^{-1}, k(T→∞) = 300 s^{-1} and E_a* = 35 cm^{-1} and the red curve with E_a = 905 cm^{-1}, k(T→∞) = 2×10^6 s^{-1} and E_a* = 75 cm^{-1}.

Light-Induced Thermal hysteresis

For cooperative compounds, it has been shown[15,33] that a permanent light irradiation upon warming an cooling can open a light-induced thermal hysteresis (LITH) due to the competition between HS → LS relaxation and LS → HS population. The LITH curve has been recorded under permanent green light irradiation at a 0.3 $Kmin^{-1}$ temperature scan rate and is presented in Figure 6a. The revealed 30 K wide hysteresis is the result of a kinetic equilibrium between relaxation and population, and the clear evidence of the opening of a hysteresis can be obtained by recording photostationary points. Figure 6b reports the results of irradiation at 45 K for 6 hrs in both the LS and the HS states. The two curves clearly do not tend to the same point, illustrating the presence of a light-induced hysteresis. Moreover, the huge difference indicates that the hysteresis is large. While it is expected for highly cooperative compounds, it is quite surprising considering the small additional activation energy values, E_a* (35 and 75 cm^{-1}). The estimation of the real hysteresis width would require time consuming experiment such as slower temperature scan rate or record of the photostationary points, which is out of the scope of this study.

Another interesting feature is that in the warming branch we observe a shoulder in the derivative curve at 58 K (arrow on Figure 5c), which is coincident with the temperature at which we propose that a phase transition occurs between two cooperative relaxation processes. The observation of this shoulder on the LITH curve and not on the *T*(LIESST) curve comes from the fact that under light irradiation the HS metastable state is favoured and the efficient thermal relaxation occurs at higher temperature (4 K higher in that case). Therefore, in the LITH curve we can overpass the *T*(LIESST) value and observe a signature of a potential phase transition between 56 and 59 K.

Conclusions

reached the *T*(LIESST) and LITH curves were recorded according to

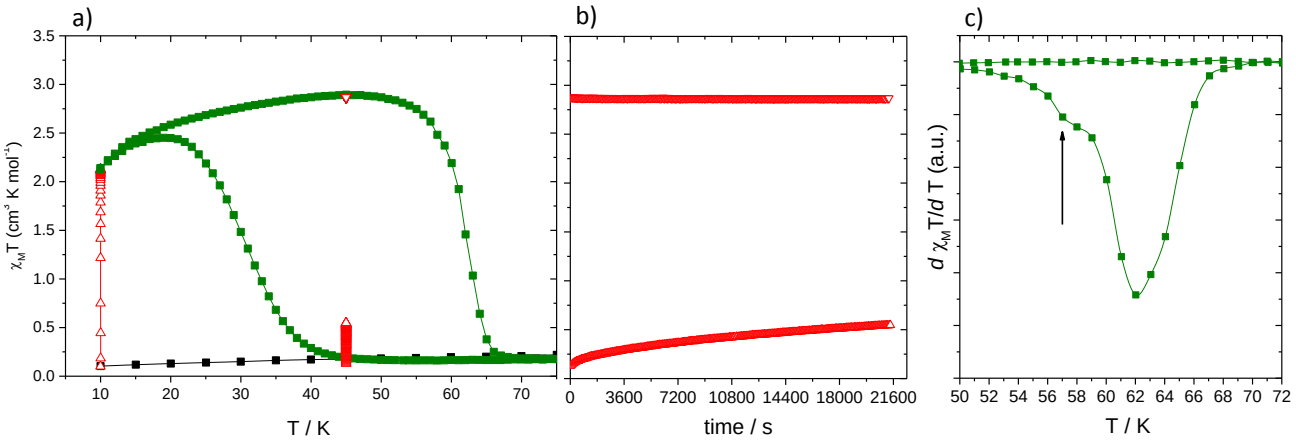

Figure 6: (a) Light-Induced Thermal Hysteresis recorded at 0.3 K min^{-1} under a permanent irradiation at 532 nm (5 mW cm^{-2}) with photostationary points (Δ and ∇) at 10 K and 45 K. (b) Temporal view of the photostationary points. (c) Derivative of χ_MT product evidencing the presence of an inflexion at 58 K (arrow).

In summary, we have characterised in detail the photomagnetic properties of a compound that exhibits a three-stepped hysteretic SCO process. The HS state can be reached at low temperature in a quantitative manner by irradiating at 514 nm. This photo-induced HS state can be depopulated by irradiation at 830 nm through the reverse-LIESST process. The *T*(LIESST) temperature was recorded and measured at 58 K. There is no evidence for any step in the *T*(LIESST) curve, as seen in the thermal SCO, with the derivative of the curve exhibiting only one minimum.

The relaxation kinetics were recorded from 40 to 62 K and fitted using several models. No steps were evidenced on the isothermal relaxation curves as clearly as on the thermal SCO. Above 50 K we observed an unusual behaviour in the Arrhenius plot since a clear change of slope occur between 56 and 59 K. Up to now changes in the lnk_{HL} vs 1/*T* curve was ascribed to the crossing between the tunnelling and the thermally activated region of the relaxation or to the overlap with the thermal hysteresis loop[34]. With the absence of any steps in the *T*(LIESST) curve, it appears likely that several HS sites are relaxing or that a structural reorganisation that takes place inducing a change in the relaxation rate. The occurrence of a possible phase transition was also confirmed by the shape of the LITH loop that shows a curvature around 58 K, a temperature at which we propose there is a transition between two cooperative phases.

Experimental Section

Photomagnetic measurements were performed on polycrystalline samples using a Spectrum Physics Series 2025 Kr$^+$ laser (514.5 nm or 647 nm at 5 mW cm^{-2}) or a 830 nm photodiode (3.5 mW cm^{-2}), coupled through an optical fibre to the cavity of a MPMS-5S Quantum Design SQUID magnetometer. The optical power at the sample surface was adjusted to prevent an important warming of the sample. The compound, which was synthesised via previously reported methods,[28] consisted of a yellow solid in ethanol/water solution. To prevent guest molecule desorption, the sample was quickly transferred from solution to grease then inserted within the sample-holder as a thin layer of sample-containing grease. Its weight (around 0.1 mg) was obtained by comparison of the thermal spin crossover curve with that of a more accurately weighted sample of the same material. After being slowly cooled at 10 K, the sample in the low-spin state was irradiated and the change in magnetic susceptibility was followed. When the saturation point was reached the *T*(LIESST) and LITH curves were recorded according to classical procedure[17-21]: a temperature increase at a rate of ~0.3 K min^{-1} with a magnetisation measurement every 1 K. All the measurements were performed at 20 kOe of applied field.

Acknowledgments

GC thanks the University of Bordeaux, the CNRS, the Aquitaine Region that supported this work. SMN and CJK thank the Australian Research Council for Discovery Project and Fellowship funding.

[1] P. Gütlich, H. A. Goodwin, (eds.), *Spin Crossover in Transition Metal Compounds I-III. Topics in Current Chemistry* vols. 233-235; Springer, Berlin, Germany, 2004.
[2] M. A. Halcrow (ed), Spin-crossover materials – properties and applications; John Wiley & Sons, Chichester, UK, 2013, p. 568.
[3] S. Bonhommeau, G. Molnar, A. Galet, A. Swick, J.A. Real, J.J. McGarvey, A. Bousseksou, *Angew. Chem. Int. Ed., Engl*, **2005**, *44*, 2.
[4] G. Gallé, C. Etrillard, J. Degert, F. Guillaume, J.-F. Létard, E. Freysz, *Appl. Phys. Lett.* **2013**, *102*, 063302.
[5] H. J. Shepherd, G. Molnár, W. Nicolazzi, L. Salmon, A. Bousseksou, *Eur. J. Inorg. Chem.* **2013**, 653.
[6] J. Linares, E. Codjovi, Y. Garcia, *Sensors*, **2012**, *12*, 4479.
[7] O. S. Wenger, *Chem. Rev*. **2013**, *113*, 3686.
[8] A. B. Gaspar, M. Seredyuk, *Coord. Chem. Rev*. **2014**, *268*, 41.
[9] M. D. Manrique-Juárez, S. Rat, L. Salmon, G. Molnár, C. M. Quintero, L. Nicu, H. J. Shepherd, A. Bousseksou, *Coord. Chem. Rev*. **2016**, *308*, 395.
[10] P. Guionneau, *Dalton Trans*. **2014**, *43*, 382
[11] (a) M. Paez-Espejo, M. Sy, K. Boukheddaden, *J. Am. Chem. Soc*. **2016**, *138*, 3202; (b) E. Trzop, D. Zhang, L. Pineiro-Lopez, F. J. Valverde-Munoz, M. Carmen Munoz, L. Palatinus, L. Guerin, H. Cailleau, J. A. Real, and E. Collet *Angew. Chem. int. Ed.* **2016**, *55*, 8675
[12] S. Decurtins, P. Gütlich, C.P Kohler, H. Spiering, A. Hauser, *Chem. Phys. Lett.* **1984**, 105, 1
[13] A. Hauser, in: P. Gütlich, H.A. Goodwin (Eds.) Spin crossover in transition metal compounds II. *Top. Curr. Chem.* **2004**, 234, 155.
[14] A. Hauser, *Chem. Phys. Lett.* **1992**, *192*, 65.
[15] A. Hauser, J. Jeftić, H. Romstedt, R. Hinek, H. Spiering, *Coord. Chem. Rev*. **1999**, *190-192*, 471.
[16] A. Hauser, C. Enachescu, M. Lawson Daku, A. Vargas, N. Amstutz, *Coord. Chem. Rev*. **2006**, *250*, 1642.
[17] J-F. Létard , P. Guionneau, L. Rabardel, J. A. K. Howard, A. Goeta, D. Chasseau, O. Kahn, *Inorg. Chem*. **1998**, *37*, 4432
[18] J-F. Létard, P. Guionneau, O. Nguyen, J. S. Costa, S. Marcen, G. Chastanet, M. Marchivie, L. Capes, *Chem. Eur. J*. **2005**, *11*, 4582
[19] S. Marcen, L. Lecren, L. Capes, H. A. Goodwin, J-F. Létard, *Chem. Phys. Lett.* **2002**, *358*, 87
[20] J.-F. Létard, *J. Mater. Chem*. **2006**, *16*, 2550.

[21] J-F. Létard, G. Chastanet, P. Guionneau, C. Desplanches in Spin-crossover materials – properties and applications, M. A. Halcrow (ed.), John Wiley & Sons, Chichester, UK, 2013, ch. 19, p. 475.
[22] J. Klingele, D. Kaase, M. Schmucker, Y. Lan, G. Chastanet, J.-F. Létard, *Inorg. Chem.* **2013**, *52*, 6000.
[23] G. Matouzenko, J.-F. Létard, S. Lecocq, A. Bousseksou, L. Capes, L. Salmon, M. Perrin, O. Kahn, A. Collet, *Eur. J. Inorg. Chem.* **2001**, 2935
[24] V. Niel, A.L. Thompson, A.E. Goeta, C. Enachescu, A. Hauser, A. Galet, M. Carmen Munoz, J.A. Real, *Chem. Eur. J.* **2005**, *11*, 2047
[25] R. Mohammed, G. Chastanet, F. Tuna, T.L. Malkin, S.A. Barrett, C.A. Kilner, J.-F. Létard, M.A. Halcrow, *Eur. J. Inorg. Chem.* **2013**, 819
[26] C. Baldé, W. Bauer, E. Kaps, S. Neville, C. Desplanches, G. Chastanet, B.Weber, J.-F. Létard, *Eur. J. Inorg. Chem.* **2013**, 2744
[27] B.A. Leita, S.M. Neville, G.J. Halder, B. Moubaraki, C.J. Kepert, J.-F. Létard, K.S. Murray, *Inorg. Chem*. **2007**, *46*, 8784
[28] M. Buron-Le Cointe, N. Ould Moussa, E. Trzop, A. Moréac, G. Molnar, L. Toupet, A. Bousseksou, J.-F. Létard, G.S. Matouzenko, *Phys. Rev. B* 2010, *82*, 214106
[29] N. Brefuel, E. Collet, H. Watanabe, M. Kojima, N. Matsumoto, L. toupet, K. Tanaka, J.-P. Tuchagues, *Chem. Eur. J.* **2010**, *16*, 14060
[30] N. F. Sciortino, K.R. Scherl-Gruenwald, G. Chastanet, G.J. Halder, K.W. Chapman, J.-F. Létard, C.J. Kepert, *Angew. Chem. Int. Ed. Engl*. **2012**, *51*, 10154.
[31] C. Enachescu, H. Constant-Machado, E. Codjovi, J. Linares, K. Boukheddaden, F. Varret, *J. Phys. Chem. Solids* **2001**, *62*, 1409
[32] a) H. Romstedt, A. Hauser, H. Spiering, *J. Phys. Chem. Solids* **1998**, *59*, 265; b) M. Nishino, K. Boukheddaden, S. Miyashita, F. Varret, *Polyhedron*, **2005**, *24*, 2852; c) C. Enachescu, J. Linares, E. Codjovi, K. Boukheddaden, F. Varret, *J. Opt. Adv. Mater*. **2003**, *5*, 261.
[33] A. Desaix, O. Roubeau, J. Jeftic, J.G. Haasnoot, K. Boukheddaden, E. Codjovi, J. Linares, M. Nogues, F. Varret, *Eur. Phys. J. B* **1998**, *6*, 183.
[34] (a) J. Degert, N. Lascoux, S. Montant, S. Létard, E. Freysz, G. Chastanet, J.-F. Letard, *Chem. Phys. Lett.* **2005**, *415*, 206; (b) N. Paradis, G. Chastanet, J.-F. Létard, *Eur. J. Inorg. Chem*. **2012**, 3618 ; (c) N. Paradis, G. Chastanet, F. Varret, J.-F. Létard, *Eur. J. Inorg. Chem*, **2013**, 968 ; (d) N. Paradis, G. Chastanet, T. Palamarciuc, P. Rosa, F. Varret, K. Boukheddaden, J.-F. Létard, *J. Phys. Chem. C*, **2015**, 119, 20039.

Received: ((will be filled in by the editorial staff))
Published online: ((will be filled in by the editorial staff))

Entry for the Table of Contents

Layout 1:

((Key Topic))

High Spin → Low Spin Relaxation Regime Change in a Multistep 3D Spin-Crossover Material.

From detailed analysis of relaxation kinetics recorded on a multistep spin crossover compound, a clear regime change is observed, hiding a probable phase transition.

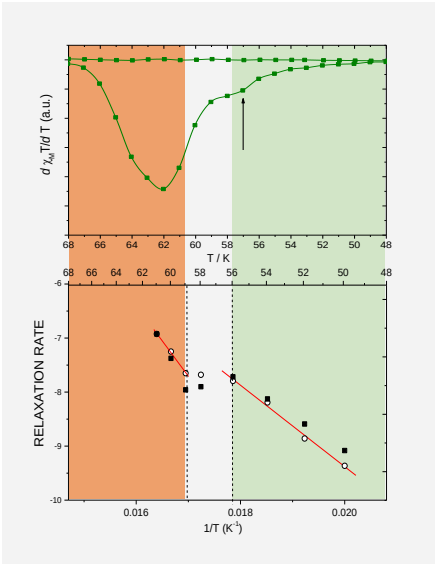

Guillaume Chastanet, Natasha F. Sciortino, Suzanne M. Neville, Cameron J. Kepert

…….. Page No. – Page No.

Keywords: Multistep spin crossover / Iron(II) / relaxation kinetics / LIESST / Photomagnetism